Available online at www.sciencedirect.com

ScienceDirect

Scripta Materialia 102 (2015) 35–38

Scripta MATERIALIA

www.elsevier.com/locate/scriptamat

New insights into phase transformations in single crystal silicon by controlled cyclic nanoindentation

Hu Huang and Jiwang Yan*

Department of Mechanical Engineering, Keio University, Yokohama 223-8522, Japan

Received 13 January 2015; accepted 1 February 2015
Available online 20 February 2015

Phase transformations in single crystal silicon were investigated by cyclic nanoindentation with controlled residual loads in the unloading process. Different phase transformations were observed at different residual loads, leading to appearance of pop-outs in different positions, which has never been reported before. Phase transformation mechanism in the reloading process was discussed by analyzing the slope change in the indentation displacement–time curve.

Keywords: Nanoindentation; Silicon; Phase transformations; Raman spectroscopy

As single crystal silicon is an important semiconductor material in scientific research and industrial applications, its mechanical properties have been a research focus for many years. Especially, interests have been concentrated in phase transformations occurring under high pressure loading and the subsequent pressure release [1–7], which affect its mechanical [8], electrical [9,10] and chemical performances [11]. Diamond anvil cell [1,3,5] and nanoindentation [2,4,6,12] are two commonly used methods to study high pressure phase transformations in single crystal silicon under a contact load. Taking advantages of high measuring resolution, small testing volume (nondestructive testing), easy to use, and good compatibility of sample size, nanoindentation has been given increasing attentions [13–17].

By combining Raman spectroscopy [16–20], transmission electron microscopy [21], in situ electrical characterization [9,10,22,23] as well as diamond anvil cell experiments, a few phase transformation mechanisms in single crystal silicon during nanoindentation have been clarified. In the loading process, crystalline silicon (c-Si) with the diamond cubic Si-I phase transforms into a much denser metallic Si-II phase (β-Sn phase) at a pressure of ~11 GPa. This transformation involves volume decrease, and may lead to discontinuities in the loading curve. In the unloading processes, phase transformations of silicon depend on the unloading conditions. For fast unloading, the Si-II phase is ready to transform gradually into amorphous silicon (a-Si), leading to obvious slope change and appearance of an elbow. For slow unloading, the Si-II phase prefers to suddenly transform into high-pressure crystalline phases Si-XII/III, leading to an obvious discontinuity in the unloading curve, namely, pop-out.

Although many studies have been reported on phase transformations both in single-cycle nanoindentation [14,17,24] and multi-cycle nanoindentation [25,26], the mechanisms and the paths of phase transformation are still poorly understood. There are still contradictions in conclusions. For example, due to the lack of direct evidence, some authors suggest that the Si-XII phase can transform into Si-II in the reloading process [27,28], but some others comment that the Si-XII phase is relatively stable and is hard to retransform into Si-II in reloading at the same indentation load [22,25,26]. Further investigations on nanoindentation induced phase transformations in single crystal silicon are necessary. In this paper, a cyclic nanoindentation protocol is introduced by controlling the residual load in the unloading process to obtain different initial phases for the next nanoindentation cycle. In this way, effects of different initial phases on phase transformation behaviors in the subsequent nanoindentation cycles can be investigated.

The single crystal silicon (1 0 0) sample used in this study was n-type boron doped with a resistivity of 2.0 ~ 8.0 Ωcm. Nanoindentation tests were performed on the ENT-1100 nanoindentation instrument (Elionix Inc., Japan) with a Berkovich indenter. For all nanoindentation tests, the maximum indentation load was the same, 50 mN. Firstly, single-cycle nanoindentation tests with a loading/unloading rate of 5 mN/s were made on twenty points to obtain the load range for pop-out occurrence in the unloading process. Obvious pop-outs appeared in 17 nanoindentation tests, and the load range for pop-out was 7 ~ 18 mN. Then, ten cyclic nanoindentation tests were carried out with the same

* Corresponding author; e-mail: yan@mech.keio.ac.jp

http://dx.doi.org/10.1016/j.scriptamat.2015.02.008
1359-6462/

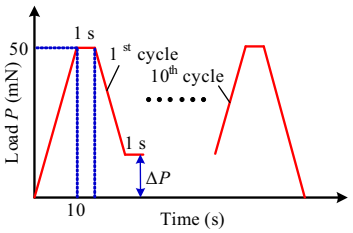

Figure 1. Schematic diagram of controlled cyclic nanoindentation.

loading/unloading rate (5 mN/s). The holding time at the maximum indentation load for all indentation tests was 1 s.

Figure 1 illustrates the experimental schematic. By controlling the residual load ΔP ($\Delta P = 0$, 8, 12, 16, 20 mN) in the unloading process, different initial phases for the next nanoindentation cycle can be obtained. For each ΔP, five group experiments were implemented, named (a-1)∼(a-5) for $\Delta P = 0$ mN, (b-1)∼(b-5) for $\Delta P = 8$ mN, (c-1)∼(c-5) for $\Delta P = 12$ mN, (d-1)∼(d-5) for $\Delta P = 16$ mN, and (e-1)∼(e-5) for $\Delta P = 20$ mN. After nanoindentation tests, residual phases of the indents were analyzed by a NRS-3000 Raman micro-spectrometer (JASCO, Japan) with a 532 nm wavelength laser focused to a ∼ 1 μm spot size.

Figure 2 gives some representative load–displacement curves. To clearly identify individual cycles, the reloading/unloading curves are shifted rightward artificially. When $\Delta P = 0$, two pop-outs appear in the first and second cycles respectively as shown in Figure 2(a) for all the five experiments (a-1)∼(a-5). A similar phenomenon is observed in Figure 2(b) and (c) when $\Delta P = 8$ mN, but a small difference appears. In Figure 2(b), the first pop-out occurs during holding. When $\Delta P = 12$, 16 and 20 mN, an interesting phenomenon, which has never been reported before, is observed that displacement decrease appears in the reloading process, as shown in Figure 2(d), (f) and (h). This kind of displacement decrease can also be treated as a pop-out because its displacement change is similar to the pop-out in unloading in Figure 2(a). In addition, in Figure 2(d) and (f), two pop-outs occur in the same nanoindentation cycle. In Figure 2(e), a pop-out is observed in the third unloading cycle. However, the second pop-out is not observed in Figure 2(e) and (h), which may be resulted from very small displacement decrease in these two unloading processes. In Figure 2(g), there is no pop-out in the first nine nanoindentation cycles, and only one pop-out appears in the last nanoindentation cycle. In Figure 2(i), there is no pop-out observed in all ten nanoindentation cycles, and an elbow appears in the last nanoindentation cycle.

Figure 3 illustrates the Raman spectra results of residual indents corresponding to experiments in Figure 2. Peaks at∼353, 384, 397, 437, and 521 cm^{-1} are observed in spectra curves (a-1)∼(e-3), but only a broadband appears in the spectra curve (e-4), as shown in the inset figures with magnified scale of Raman intensity. According to Ref [20], the peak at 521 cm^{-1} corresponds to the Si-I cubic diamond structure, peaks at ∼ 350, 397 and 435 cm^{-1} correspond to the Si-XII phase and the peak at ∼ 382 cm^{-1} corresponds to the Si-III phase. Therefore, in the residual indents of experiments (a-1)∼(e-3), the dominated end phases are a mixture of Si-XII/Si-III phases, while amorphous silicon (*a*-Si) dominates the end phase of the residual indent in

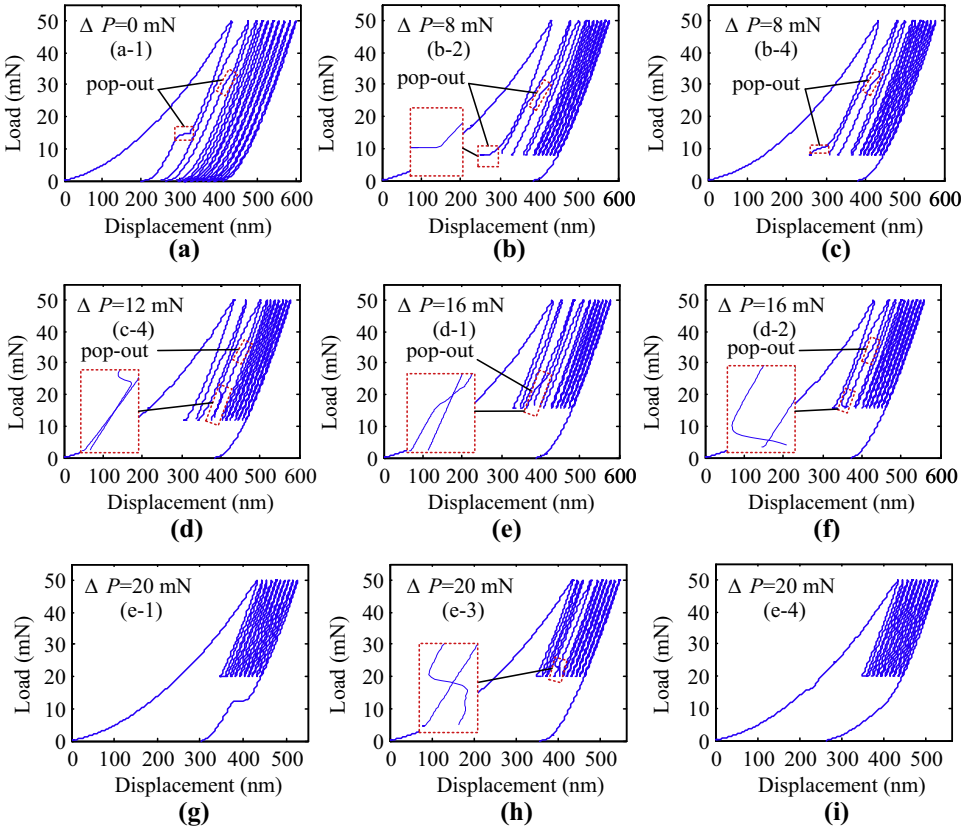

Figure 2. Some representative results of cyclic nanoindentation by controlling the residual loads: (a) $\Delta P = 0$ mN; (b and c) $\Delta P = 8$ mN; (d) $\Delta P = 12$ mN; (e and f) $\Delta P = 16$ mN; (g, h and i) $\Delta P = 20$ mN.

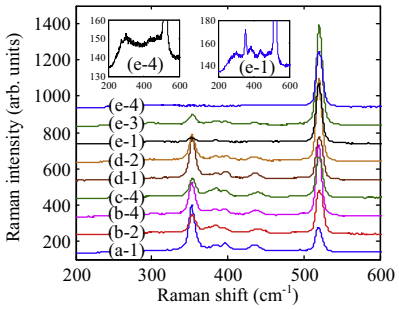

Figure 3. Raman spectra obtained from residual indents corresponding to the cyclic nanoindentation experiments in Figure 2.

the experiment (e-4). The peak shift in Figure 3 is mainly resulted from residual stress in the indents. From Figure 3, a conclusion can be derived that though the position of pop-out occurrence (unloading process, holding process, or reloading process) and the number of pop-out (one or two) are different, as shown in Figure 2, the dominated end phases are the same once the pop-out happens.

Phase transformations of single crystal silicon usually involve significant volume change, resulting in obvious discontinuities in the load–displacement curve [2,9]. For example, the cubic diamond structure Si-I phase transforms into a much denser metallic Si-II phase, leading to ~22% volume decrease of the transformed materials. Thus, the pop-in may appear in the loading process. The Si-II phase transforms into the *a*-Si phase or the Si-XII phase with ~ 24% or ~ 9% volume expansion respectively, leading to appearance of the elbow or pop-out. Large volume changes will be shown directly in the indentation displacement curves. In this study, an analysis method based on indentation displacement–time curve is used to reveal the phase transformation mechanism in Figure 2.

Figure 4(a) and (b) illustrates displacement–time curves of experiments (c-4) and (e-3) respectively. In these two experiments, pop-outs appeared in the reloading process, as shown in Figure 2. Corresponding to the pop-outs, displacement decrease was observed in the third reloading process in experiment (c-4) and the fourth reloading process in experiment (e-3), indicating that volume underneath the indenter suddenly expands. Considering that there is no new phase formed, displacement decrease in the reloading processes in Figure 4 demonstrates that the Si-II phase is transforming into the Si-XII phase.

From the inset figure in Figure 4(b), interaction between the indenter and the specimen during the phase transformation process can be analyzed in detail. The forth reloading process in experiment (e-3) can be divided into five steps as shown in Figure 4(b). Because there is no pop-out in the first three nanoindentation cycles, the dominated initial phase for the fourth cycle is Si-II, with a small volume of the Si-I phase. In step I, the indenter penetrates into the residual indent again at 46 s according to the control strategy shown in Figure 1, and penetration displacement gradually increases. In step II, transformation from the Si-II phase to the Si-XII phase begins at ~ 46.18 s, and volume underneath the indenter expands, leading to the uplift of material under the indenter which can further lead to an increase of the penetrate load. In step II, penetration displacement nearly keeps a constant until ~ 46.46 s. In step III, penetration displacement quickly decreases due to volume markedly expanding underneath the indenter, and it continues until ~ 46.66 s at which transformation from the Si-II phase to the Si-XII phase nearly finishes. From steps II and III, Si-II to Si-XII transformation time of ~ 0.48 s is calculated. After step III, silicon underneath the indenter is a mixture of Si-II, Si-XII and Si-I phases. In step IV, penetration displacement approximatively linearly increases with increase of time, demonstrating that the material underneath the indenter nearly deforms elastically. At ~ 50.7 s, the slope of the displacement–time curve obviously increases, which means volume underneath the indenter suddenly decreases and the denser phase is formed again. With consideration of the density relationships between different phases (Si-I < Si-II, Si-XII < Si-II), there are two possible phase transformation processes leading to volume decrease suddenly. One is Si-XII formed in steps II and III retransforming to Si-II [27,28]. The other is the residual Si-I phase transforming to Si-II. However, in the subsequent nanoindentation cycles, sudden changes of the slope in the reloading displacement–time curves are not observed. If step V is resulted from the Si-XII to Si-II transformation, it can also happen in the subsequent cycles because they have similar indentation-induced high pressure processes. So, increase of the slope in the initial of step V is due to phase transformation from the residual Si-I phase to Si-II. With increase of the time, the transformation process gradually finishes and the slope gradually decreases again. In the subsequent reloading cycles, there is nearly no Si-I in the indentation affecting region and thus obvious slope change does not appear again.

Similar phase transformation processes can be observed in the third reloading process in the experiment (c-4) as shown in Figure 4(a). A small difference also appears that step II is not obvious in Figure 4(a), and the Si-II to Si-XII transformation time is ~ 0.18 s which is obviously smaller than that in Figure 4(b). This leads to the phase

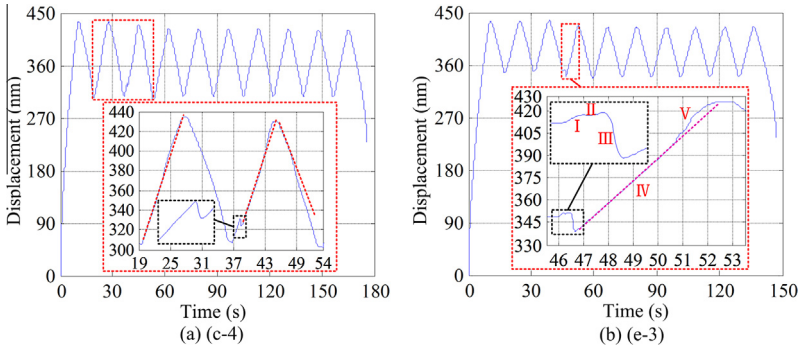

Figure 4. Displacement vs. time in controlled cyclic nanoindentation tests of (a) (c-4) and (b) (e-3).

transformation from Si-II to Si-XII being not fully finished and thus obvious change of the slope is observed in the third unloading process in Figure 4(a), corresponding to the pop-out in the unloading curve in Figure 2(d). This further explains why the second pop-out is not obviously observed in Figure 2(h).

In summary, controlled cyclic nanoindentation tests were carried out on single crystal silicon. By controlling the residual load in the unloading process, pop-outs appeared at different positions, namely, the unloading process, the holding process and the reloading process. The pop-out occurring in the reloading process indicates a phase transformation from Si-II to Si-XII in a pressure loading process, which has never been reported before. Phase transformation mechanism for the pop-out in the reloading process was analyzed by the slope change in the displacement–time curves. This work enhances the understanding of high pressure phase transformation paths and mechanisms of single crystal silicon.

H.H. as an International Research Fellow of the Japan Society for the Promotion of Science (JSPS) acknowledges the financial support from JSPS (Grant No. 26-04048).

[1] R.O. Piltz, J.R. Maclean, S.J. Clark, G.J. Ackland, P.D. Hatton, J. Crain, Phys. Rev. B 52 (1995) 4072.
[2] V. Domnich, Y. Gogotsi, Rev. Adv. Mater. Sci. 3 (2002) 1.
[3] J. Crain, G.J. Ackland, J.R. Maclean, R.O. Piltz, P.D. Hatton, G.S. Pawley, Phys. Rev. B 50 (1994) 13043.
[4] I. Zarudi, L.C. Zhang, J. Zou, T. Vodenitcharova, J. Mater. Res. 19 (2004) 332.
[5] B. Haberl, M. Guthrie, D.J. Sprouster, J.S. Williams, J.E. Bradby, J. Appl. Crystallogr. 46 (2013) 758.
[6] Z.D. Zeng, Q.S. Zeng, W.L. Mao, S.X. Qu, J. Appl. Phys. 115 (2014) 103514.
[7] M.I. Mcmahon, R.J. Nelmes, N.G. Wright, D.R. Allan, Phys. Rev. B 50 (1994) 739.
[8] J.W. Yan, H. Takahashi, J. Tamaki, X.H. Gai, H. Harada, J. Patten, Appl. Phys. Lett. 86 (2005) 181913.
[9] J.E. Bradby, J.S. Williams, M.V. Swain, Phys. Rev. B 67 (2003) 085205.
[10] S. Ruffell, J.E. Bradby, N. Fujisawa, J.S. Williams, J. Appl. Phys. 101 (2007) 083531.
[11] S.W. Youn, C.G. Kang, Scr. Mater. 50 (2004) 105.
[12] A. Kailer, Y.G. Gogotsi, K.G. Nickel, J. Appl. Phys. 81 (1997) 3057.
[13] L.B.B. Aji, S. Ruffell, B. Haberl, J.E. Bradby, J.S. Williams, J. Mater. Res. 28 (2013) 1056.
[14] L. Chang, L.C. Zhang, Acta Mater. 57 (2009) 2148.
[15] Y.B. Gerbig, S.J. Stranick, D.J. Morris, M.D. Vaudin, R.F. Cook, J. Mater. Res. 24 (2009) 1172.
[16] T. Juliano, Y. Gogotsi, V. Domnich, J. Mater. Res. 18 (2003) 1192.
[17] T. Juliano, V. Domnich, Y. Gogotsi, J. Mater. Res. 19 (2004) 3099.
[18] Y.B. Gerbig, C.A. Michaels, R.F. Cook, J. Mater. Res. (2014), http://dx.doi.org/10.1557/jmr.2014.316.
[19] Y.B. Gerbig, C.A. Michaels, A.M. Forster, R.F. Cook, Phys. Rev. B 85 (2012) 104102.
[20] P.S. Pizani, R.G. Jasinevicius, A.R. Zanatta, Appl. Phys. Lett. 89 (2006) 031917.
[21] I. Zarudi, J. Zou, L.C. Zhang, Appl. Phys. Lett. 82 (2003) 874.
[22] S. Ruffell, J.E. Bradby, J.S. Williams, P. Munroe, J. Appl. Phys. 102 (2007) 063521.
[23] S. Ruffell, J.E. Bradby, J.S. Williams, O.L. Warren, J. Mater. Res. 22 (2007) 578.
[24] J.W. Yan, H. Takahashi, X.H. Gai, H. Harada, J. Tamaki, T. Kuriyagawa, Mater. Sci. Eng. A, Struct. 423 (2006) 19.
[25] N. Fujisawa, S. Ruffell, J.E. Bradby, J.S. Williams, B. Haberl, O.L. Warren, J. Appl. Phys. 105 (2009) 106111.
[26] N. Fujisawa, J.S. Williams, M.V. Swain, J. Mater. Res. 22 (2007) 2992.
[27] S.R. Jian, G.J. Chen, J.Y. Juang, Curr. Opin. Solid St. M. 14 (2010) 69.
[28] V. Domnich, Y. Gogotsi, M. Trenary, MRS Proc. 649 (2000), Q 8.9.